Chinese Chemical Letters 24 (2013) 307–310

Contents lists available at SciVerse ScienceDirect

Chinese Chemical Letters

journal homepage: www.elsevier.com/locate/cclet

Original article

Effects of Mo promoters on the Cu–Fe bimetal catalysts for the DMC formation from CO_2 and methanol

Ying-Jie Zhou [a], Min Xiao [a,*], Shuan-Jin Wang [a], Dong-Mei Han [a], Yi-Xin Lu [b], Yue-Zhong Meng [a,*]

[a] The Key Laboratory of Low-carbon Chemistry & Energy Conservation of Guangdong Province/State Key Laboratory of Optoelectronic Materials and Technologies, Sun Yat-sen University, Guangzhou 510275, China
[b] Department of Chemistry & Medicinal Chemistry Program, Office of Life Sciences, National University of Singapore, Singapore 117543, Republic of Singapore

ARTICLE INFO

Article history:
Received 31 December 2012
Received in revised form 21 January 2013
Accepted 24 January 2013
Available online 14 March 2013

Keywords:
Dimethyl carbonate
Carbon dioxide
Catalysis
Bimetal catalyst

ABSTRACT

The Mo-promoted Cu–Fe bimetal catalysts were prepared and used for the formation of dimethyl carbonate (DMC) from CO_2 and methanol. The catalysts were characterized by X-ray diffraction (XRD), temperature programmed reduction (TPR), laser Raman spectra (LRS), energy dispersive spectroscopy (EDS) and temperature programmed desorption (TPD) techniques. The experimental results demonstrated that the Mo promoters can decrease the reducibility and increase the dispersion of Cu–Fe clusters. The concentration balance of base–acid sites can be readily adjusted by changing the Mo content. The moderate concentration balance of acid and base sites was in favor of the DMC formation. Under optimal experimental conditions, the highest methanol conversion of 6.99% with a DMC selectivity of 87.7% can be obtained when 2.5 wt% of Mo was loaded.

1. Introduction

The incorporation of carbon dioxide (CO_2) into industrially useful organic products is receiving significant attention as CO_2 is abundant, inexpensive and non-toxic [1]. One of the promising reactions in this area is the direct synthesis of dimethyl carbonate (DMC) from CO_2 and methanol [2]. DMC has increasingly attracted interest for its benign nature and wide applications. It is used as an alternative to the notorious phosgene in several organic transformations [3], starting materials for polycarbonates resin, electrolyte of lithium-ion batteries, an octane booster in gasoline and so on [4].

In recent years, a variety of catalysts for this reaction have been investigated, such as organometallic compounds [5], metal (IV) tetra alkoxide [6], potassium carbonate [7], zirconia-based [8–10] catalysts, cerium-based [11,12] catalysts, heteropoly compounds [13], H_3PO_4–V_2O_5 [14], Cu–Ni bimetallic [15–18] supported on different carriers. However, these catalysts suffer from tedious preparation procedures or agglomeration of active components, which might restrict their effective use and wide application from the industrial point of view. Transition group elements have drawn considerable attention to interact with CO_2 because of their unusual electronic structures and ability to enhance catalytic properties [19]. In our previous study, we have investigated the Cu–Fe bimetal catalysts in the direct DMC formation from CO_2 and methanol. It was found that catalysts with moderate molar ratios of acid–base sites were in favor of the DMC formation [20]. However, the DMC yields were not very satisfactory, and the development of catalyst that combined large amount of acid and base sites with desirable catalytic activity was necessary. On the other hand, the addition of a second or third metal component to a catalyst will improve the dispersion or alter the electronic structure of a catalyst. More importantly, the presence of a promoter can modify the adsorption characteristics of the catalyst surface, change the reducibility of the catalyst or in certain cases alter the catalytic performance [21]. There have been many papers reporting the effects of Mo as a structural promoter on catalytic properties of Fe-based catalysts [22–24]. The addition of Mo has beneficial effects on the stabilization and dispersion of iron on the catalyst support. Moreover, the intrinsic acid–base sites on molybdenum oxides could enhance the reactions. Therefore, it could be expected that the addition of molybdenum to a Cu–Fe catalyst might have potential advantages for the DMC formation from CO_2 and methanol. In this contribution, the Mo-promoted Cu–Fe bimetal catalysts were prepared and evaluated for the DMC formation from CO_2 and methanol. The effects of Mo contents on the activity and structure of the catalysts are reported.

* Corresponding authors.
E-mail addresses: stsxm@mail.sysu.edu.cn (M. Xiao), mengyzh@mail.sysu.edu.cn (Y.-Z. Meng).

1001-8417/$ – see front matter © 2013 Min Xiao. Published by Elsevier B.V. on behalf of Chinese Chemical Society. All rights reserved.
http://dx.doi.org/10.1016/j.cclet.2013.02.001

2. Experimental

2.1. Catalyst preparation

Mo-promoted Cu–Fe-based catalysts were prepared in two steps. First, Mo was loaded on silica (China GBS Hightech &Industry Co., Ltd., HL-380) using wet impregnation methods. Appropriate amounts of $(NH_4)_6Mo_7O_{24}{\cdot}4H_2O$ were dissolved in deionized water and impregnated over silica. The samples were then dried in a rotary evaporator and calcined at 500 °C for 5 h to yield the xMo/SiO_2 (x = 1, 2.5, 4, 5.5 or 7 wt%). Afterward, the Cu–Fe bimetal (CuO + Fe_2O_3 = 15 wt%, Cu:Fe = 3:2) were loaded on xMo/SiO_2 using the citric acid method [25]. An aqueous solution of citric acid and the metal precursors such as iron nitrate, copper nitrate were impregnated over xMo/SiO_2, followed by heating at 60 °C for 1 h until the mixture became gelatinous. The as-prepared samples were dried at 120 °C overnight before being subjected to calcinations at 500 °C in air for 4 h. All catalysts were reduced in a hydrogen stream at 600 °C for 4 h, prior to each catalytic measurement.

2.2. Catalyst characterizations

Powder X-ray diffraction (XRD) measurements were performed on a Rigaku D-Max 2200 diffractometer using graphite-filtered Cu K_α radiation (λ = 0.154178 nm) at 40 kV and 30 mA. The crystallite size of the particles was estimated from the XRD peak widths using the Scherer equation. The temperature programmed reduction (TPR) profiles of calcined catalyst precursors were recorded on a Quantachrom Chem-BET 3000 apparatus. About 50 mg sample placed in a quartz U-shaped tube was pretreated at 300 °C for 1 h in a flow of N_2 (60 mL/min) to remove the adsorbed water and other contaminants followed by cooling to 30 °C. The reducing gas 5% H_2/N_2 was passed through the samples at a flow rate of 80 mL/min, with a rate of temperature rise of 8 °C/min to 750 °C. The signal of H_2 consumption by the samples with increasing temperatures was recorded by a thermal conductivity detector (TCD). The laser Raman spectra (LRS) of the catalysts was obtained on a laser Raman apparatus (Renoshaw inVia) with a 514.5 nm line of an Ar^+ laser as the excitation source. The as-prepared catalysts were analyzed by an energy dispersive spectroscopy (EDS) in order to confirm the elements on the catalyst surface. The samples were placed on conductive double-faced tape and then placed in a scanning electron microscopy (JSM-5600LV system of JEOL) equipped with an energy dispersive X-ray detector. The accelerating voltage was 15 kV. The temperature programmed desorption (TPD) experiments were carried out on a Quantachrom Chem-BET 3000 apparatus. A flow (50 mL/min) of adsorbate gas (pure CO_2 or NH_3) was introduced into the U-shape quartz filled with 100 mg of reduced catalyst at 50 °C for 1 h, and then the degassing process was performed at a heating rate of 8 °C/min under N_2 flow (30 mL/min), and CO_2 or NH_3 desorbed was detected by a TCD.

2.3. Catalytic reactions

Catalytic activity tests were performed in a continuous tubular fixed-bed micro-reactor with catalyst weight of 2 g. Pure N_2 was fed into the reactor to exhaust the air inside before the catalyst bed was heated to the desired temperature. Methanol was introduced by passage of the CO_2 carrier gas through a saturator maintained at 35 °C. Methanol-saturated CO_2 stream was heated in a pre-heater before it was passed into the reactor. The formation of DMC from CO_2 and methanol was carried out subsequently under the following reaction conditions: pressure (P): 0.6 MPa, temperature (T): 120 °C, space velocity (SV): 360 h^{-1}. All the effluent gases were analyzed by gas chromatographs (GC) equipped with a flame ionization detector (FID). The condensed liquid collected by the cooling separator was analyzed by a gas chromatograph mass spectrometer (GCMS-QP2010 plus) to confirm the DMC formation in this reaction. The main reaction products of CO_2 reacting with methanol over the catalysts were DMC and H_2O, and there were several by-products such as CH_2O, CO and dimethyl ether (DME). The detailed description of the reactor and product analysis have been provided elsewhere [20].

3. Results and discussion

3.1. Catalytic activity

The catalytic performances and EDS results of the Mo-promoted 3Cu–2Fe/SiO_2 catalysts in the DMC formation from CO_2 and methanol are shown in Table 1. The addition of Mo element could significantly improve the catalytic performance of the Cu–Fe bimetal catalysts, and with an increase of Mo element loading contents up to 2.5 wt%, the methanol conversion increased to a maximum methanol conversion of 6.99% with a DMC selectivity of 87.7%. Further increasing Mo loading contents led to a decrease in methanol conversion. Compared to the unpromoted 3Cu–2Fe/SiO_2, the DMC selectivity was improved at low Mo contents, but gradually decreased with the increase of Mo element contents. The EDS results of the catalysts were slightly lowered than the nominal loaded contents in the synthetic route, but probably within the range of experimental error.

3.2. Catalyst structure characterizations

The presence of any crystalline phases in the catalysts characterized by XRD is shown in Fig. 1. When the Mo-promoted catalyst precursor was calcined (Fig. 1(a)), copper and iron oxides showed highly crystallized monoclinic CuO, rhombohedral α-Fe_2O_3 and orthorhombic MoO_3. For all catalysts with various Mo loading contents (Fig. 1(b)–(g)), three main peaks located at around 2θ = 43.2°, 50.4° and 74.1° were attributed to the characteristic diffraction of metallic Cu, while two broad peaks located at around 2θ = 35.5°, 62.5° were assigned to the diffraction

Table 1
The dependence of catalytic performances and surface properties on Mo contents over the catalysts[a].

Mo contents (%)	Methanol conversion (%)	DMC selectivity (%)	DMC yield (%)	EDS[b]		
				Cu	Fe	Mo
0	4.72	4.08	86.5	7.11	4.08	0
1	5.59	5.05	90.4	7.03	4.04	0.91
2.5	6.99	6.13	87.7	6.95	3.89	2.32
4	6.24	5.35	85.8	6.84	3.78	3.86
5.5	5.87	4.96	84.6	6.71	3.67	5.29
7	5.31	4.42	83.3	6.38	3.78	6.73

[a] All catalysts were reduced in H_2 stream at 600 °C for 4 h. Reaction conditions: catalyst weight: 2 g; P = 0.6 MPa, T = 120 °C, SV = 360 h^{-1}; time on stream: 7 h. The data are the peak values obtained with time on stream.
[b] Five parts of each sample was analyzed by EDS. The data were the average values.

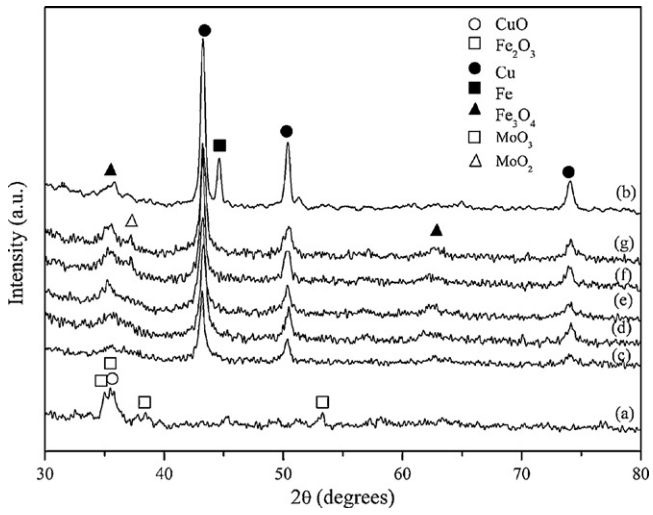

Fig. 1. XRD patterns of 3Cu–2Fe/SiO_2 with varying Mo contents before and after being reduced at 600 °C: (a) catalyst precursor calcined at 500 °C, (b) 3Cu–2Fe/SiO_2, (c) 3Cu–2Fe–1Mo/SiO_2, (d) 3Cu–2Fe–2.5Mo/SiO_2, (e) 3Cu–2Fe–4Mo/SiO_2, (f) 3Cu–2Fe–5.5Mo/SiO_2, (g) 3Cu–2Fe–7Mo/SiO_2.

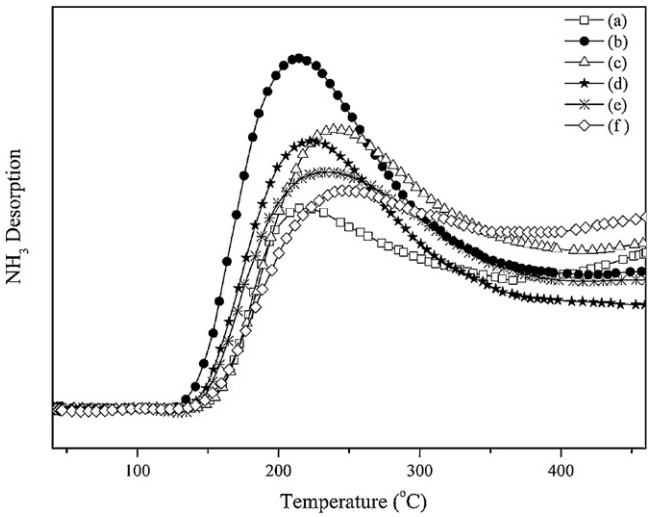

Fig. 2. TPD–NH_3 profiles of 3Cu–2Fe/SiO_2 with varying Mo contents: (a) 3Cu–2Fe/SiO_2 (b) 3Cu–2Fe–1Mo/SiO_2, (c) 3Cu–2Fe–2.5Mo/SiO_2, (d) 3Cu–2Fe–4Mo/SiO_2, (e) 3Cu–2Fe–5.5Mo/SiO_2, (f) 3Cu–2Fe–7Mo/SiO_2.

of Fe_3O_4 species. There was a peak related to metallic Fe ($2\theta = 44.6^\circ$) in the XRD pattern of 3Cu–2Fe/SiO_2 (Fig. 1(b)) but none in the Mo promoted catalysts (Fig. 1(c)–(g)). This demonstrates that the strong interactions between Cu–Fe and Mo/SiO_2 may hinder the reduction of the metal oxides to metallic particles. These can also be observed in TPR and LRS (See Figs. S1 and S2 in supporting information). No Mo phase was observed in the XRD patterns of the Mo-promoted 3Cu–2Fe/SiO_2 at lower Mo contents (Fig. 1(c)–(e)), indicating that Mo elements were highly dispersed on the SiO_2. Increasing Mo contents to above 5.5 wt% (Fig. 1(f)–(g)) led to new diffraction peaks ascribed to MoO_2 ($2\theta = 36.5^\circ$), suggesting the reduction of MoO_3 to MoO_2 in H_2 stream at 600 °C occurred. It was reported that the mixture of Fe_2O_3 and MoO_3 can form a ferric molybdate ($Fe_2(MoO_4)_3$) when calcined above 470 °C [23]. However, in this study, the molybdenum oxide was well dispersed on SiO_2 so that it was difficult to confirm the existence of ferric molybdate in the Mo-promoted 3Cu–2Fe/SiO_2. Fig. 1 also presents the changes in diffraction peaks of the active phases with different Mo loading contents. The addition of Mo to 3Cu–2Fe/SiO_2 catalysts significantly induced the broadening of the diffraction peaks of Cu and Fe species owing to the decrease in the size of the crystalline particles. This indicates a better dispersion of Cu–Fe clusters in the Mo-promoted catalysts compared to the unpromoted catalysts, which can also be observed from the TPR curves (see Fig. S1 in supporting information). The diffraction peaks became sharper when the Mo loading increased, suggesting that the Cu–Fe particles became larger with increased Mo contents. The crystalline particle sizes that are estimated from Fig. 1 using Scherrer equation are shown in Table 2. Apparently, Mo promoter can improve the dispersions of Cu–Fe phases on the catalyst, but excessive Mo loading inhibits the dispersion of Cu–Fe clusters.

The acid–base properties of the Mo-promoted 3Cu–2Fe/SiO_2 investigated by the TPD technique are shown in Fig. 2 (TPD–NH_3) and Fig. 3 (TPD–CO_2), respectively. There is one broad peak of NH_3 desorption at 150–400 °C in the TPD–NH_3 profiles over all catalysts, corresponding to one type of acid sites. The peak areas of 3Cu–2Fe/SiO_2 are lower than that of all Mo-promoted catalysts.

The addition of Mo element can effectively enhance the acid sites of the 3Cu–2Fe/SiO_2. The peak areas of NH_3 desorption decreased with increased Mo contents in 3Cu–2Fe/SiO_2, indicating that the concentration of acid sites declined at higher Mo contents. In the TPD–CO_2 profiles (Fig. 3), the peaks at around 300 °C and 460 °C were broader and more intense compared to that at 120 °C. This reveals the abundant and strong base sites on the surface of catalysts. With the increase of Mo contents in catalysts, the amount of CO_2 desorbed at 120 °C increased progressively, while desorption at 300 °C and 460 °C did not change significantly. According to the XRD (Fig. 1) studies, there existed metallic Cu, Fe_3O_4 and MoO_2 on the surface of the Mo-promoted 3Cu–2Fe/SiO_2 catalysts. The composition of the catalysts implied that there were three types of active centers on the surface of catalysts: metal sites (Cu), Lewis acid sites (Mo^{n+}, Fe^{n+}) and Lewis base sites (Mo–O, Fe–O). The enhanced acidity of the

Table 2
Crystalline particle sizes of the 3Cu–2Fe/SiO_2 with different Mo loading contents.

Mo loading (wt%)	0	1	2.5	4	5.5	7
Fe_3O_4[a] (nm)		14.4	16.3	18.9	21.6	23.5
Cu[b] (nm)	25.0	15.3	17.8	19.1	20.4	21.8

[a] 2θ values are 35.5° and 62.5°.
[b] 2θ values are 43.2°, 50.4° and 74.1°.

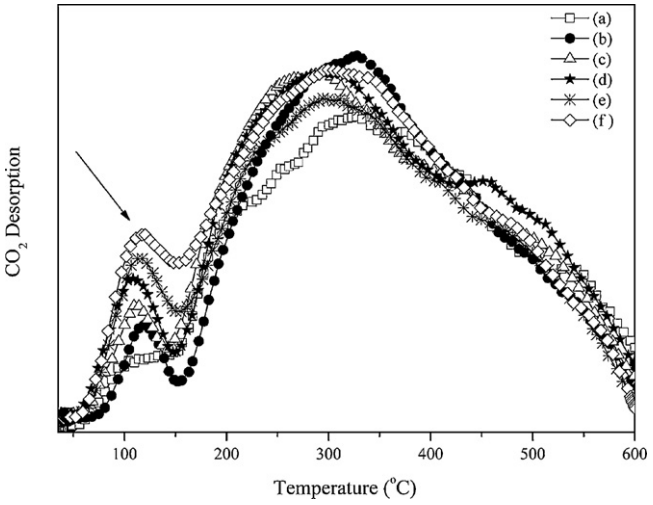

Fig. 3. TPD–CO_2 profiles of 3Cu–2Fe/SiO_2 with varying Mo contents: (a) 3Cu–2Fe/SiO_2 (b) 3Cu–2Fe–1Mo/SiO_2, (c) 3Cu–2Fe–2.5Mo/SiO_2, (d) 3Cu–2Fe–4Mo/SiO_2, (e) 3Cu–2Fe–5.5Mo/SiO_2, (f) 3Cu–2Fe–7Mo/SiO_2.

Mo-promoted Cu–Fe/SiO_2 are due to the presence of Lewis acid sites Mo^{n+}, and the enhanced basicity of the catalysts are the results of Lewis base sites Mo–O. The TPD results suggested that the introduction of the Mo afforded both extra base sites and extra acid sites for the 3Cu–2Fe/SiO_2, and it provided more base sites instead of acid sites with higher Mo loading contents.

According to the reaction mechanisms [15,26], methanol was activated on Lewis base sites to form the methoxy species and Lewis acid sites to form methyl species. The methoxy species first reacted with horizontally adsorbed CO_2 on base sites to produce the methoxy carbonate anion, which may further react with methyl species to generate the DMC. That is to say, more base sites are beneficial for the activation of CO_2 while both addition of both Lewis acid sites and Lewis base sites favors the activation of methanol. The acid and base sites of catalysts play significant roles in the catalytic performance in the DMC formation from CO_2 and methanol. Attempts were made to correlate the catalytic activity (Table 1) and acid–base properties (Figs. 2 and 3) of the catalysts. All Mo-promoted 3Cu–2Fe/SiO_2 exhibited better catalytic activity for the direct DMC formation than the unpromoted catalysts. This implies that the catalytic performance improved with an increased total number of acid and base sites. However, a no-linear correlation between catalytic activity and acid–base concentrations was observed. The catalytic performances of Mo-promoted Cu–Fe/SiO_2 first increased and then decreased with increased concentrations of base sites, but the correlation between catalytic performances and the number of acid sites present a reverse trend. Among the catalysts tested, 3Cu–2Fe–2.5Mo/SiO_2 with neither the largest basicity nor the largest acidity showed the best catalytic performance. In conclusion, the catalysts own a large amount of acid and base sites with proper ratios of acid sites to base sites favors the DMC formation.

4. Conclusion

Mo-promoted Cu–Fe based catalysts can be used in the DMC formation from CO_2 and gaseous methanol. The introduction of Mo substantially increased the dispersion of Cu–Fe clusters on support, whilst the strong interactions between the metal oxides and Mo shifted the reduction to higher temperatures. TPD results showed that the concentration of base sites increased with increased Mo contents, and suitable concentration balance of acid and base sites favors DMC formation. Under the optimal reaction conditions (120 °C, 0.6 MPa, SV = 360 h^{-1}), the introduction of Mo significantly enhanced the catalytic activity of the Cu–Fe bimetal catalysts. The highest methanol conversion of 6.99% with a DMC selectivity of 87.7% can be obtained when 2.5 wt% Mo was loaded.

Supplementary material

The reduction behaviors and the information about interactions of active metals with support of catalysts characterized by TPR and LRS are presented in supporting information.

Acknowledgments

The authors would like to thank the China High-Tech Development 863 Program (No. 2009AA03Z340), Guangdong Province Universities and Colleges Pearl River Scholar Funded Scheme (2010), Guangdong Province Sci & Tech Bureau (Key Strategic Project Nos. 2008A080800024 and 10151027501000096), and Chinese Universities Basic Research Founding for financial support of the work. Y. L. thanks National University of Singapore for financial support.

Appendix A. Supplementary data

Supplementary data associated with this article can be found, in the online version, at http://dx.doi.org/10.1016/j.cclet.2013.02.001.

References

[1] E. Leino, P. Maki-Arvela, V. Eta, et al., Conventional synthesis methods of short-chain dialkylcarbonates and novel production technology via direct route from alcohol and waste CO_2, Appl. Catal. A – Gen. 383 (2010) 1–13.
[2] N.S. Isaacs, B. O'Sullivan, C. Verhaelen, High pressure routes to dimethyl carbonate from supercritical carbon dioxide, Tetrahedron 55 (1999) 11949–11956.
[3] Y. Ono, Catalysis in the production and reactions of dimethyl carbonate, an environmentally benign building block, Appl. Catal. A – Gen. 155 (1997) 133–166.
[4] D. Delledonne, F. Rivetti, U. Romano, Developments in the production and application of dimethylcarbonate, Appl. Catal. A – Gen. 221 (2001) 241–251.
[5] J. Kizlink, Synthesis of dimethyl carbonate from carbon dioxide and methanol in the presence of organotin compounds, Collect. Czech. Chem. Commun. 58 (1993) 1399–1402.
[6] J. Kizlink, I. Pastucha, Preparation of dimethyl carbonate from methanol and carbon dioxide in the presence of Sn(IV) and Ti(IV) alkoxides and metal acetates, Collect. Czech. Chem. Commun. 60 (1995) 687–692.
[7] M.M. Du, Q.X. Li, W.T. Dong, T. Geng, Y.J. Jiang, Synthesis of glycerol carbonate from glycerol and dimethyl carbonate catalyzed by K_2CO_3/MgO, Res. Chem. Intermed. 38 (2012) 1069–1077.
[8] K. Tomishige, T. Sakaihori, Y. Ikeda, K. Fujimoto, A novel method of direct synthesis of dimethyl carbonate from methanol and carbon dioxide catalyzed by zirconia, Catal. Lett. 58 (1999) 225–229.
[9] Y. Ikeda, T. Sakaihori, K. Tomishige, K. Fujimoto, Promoting effect of phosphoric acid on zirconia catalysts in selective synthesis of dimethyl carbonate from methanol and carbon dioxide, Catal. Lett. 66 (2000) 59–62.
[10] K. Tomishige, Y. Furusawa, Y. Ikeda, M. Asadullah, K. Fujimoto, CeO_2–ZrO_2 solid solution catalyst for selective synthesis of dimethyl carbonate from methanol and carbon dioxide, Catal. Lett. 76 (2001) 71–74.
[11] M. Aresta, A. Dibenedetto, C. Pastore, et al., Cerium(IV)oxide modification by inclusion of a hetero-atom: a strategy for producing efficient and robust nano-catalysts for methanol carboxylation, Catal. Today 137 (2008) 125–131.
[12] M. Aresta, A. Dibenedetto, C. Pastore, et al., Influence of Al_2O_3 on the performance of CeO_2 used as catalyst in the direct carboxylation of methanol to dimethylcarbonate and the elucidation of the reaction mechanism, J. Catal. 269 (2010) 44–52.
[13] L.A. Allaoui, A. Aouissi, Effect of the Bronsted acidity on the behavior of CO_2 methanol reaction, J. Mol. Catal. A – Chem. 259 (2006) 281–285.
[14] X.L. Wu, M. Xiao, Y.Z. Meng, Y.X. Lu, Direct synthesis of dimethyl carbonate on H_3PO_4 modified V_2O_5, J. Mol. Catal. A – Chem. 238 (2005) 158–162.
[15] S.H. Zhong, H.S. Li, J.W. Wang, X.F. Xiao, Cu–Ni/V_2O_5–SiO_2 catalyst for the direct synthesis of dimethyl carbonate from carbon dioxide and methanol, Acta Phys. Chim. Sin. 16 (2000) 226–231.
[16] X.J. Wang, M. Xiao, S.J. Wang, Y.X. Lu, Y.Z. Meng, Direct synthesis of dimethyl carbonate from carbon dioxide and methanol using supported copper (Ni, V, O) catalyst with photo-assistance, J. Mol. Catal. A – Chem. 278 (2007) 92–96.
[17] J. Bian, M. Xiao, S.J. Wang, Y.X. Lu, Y.Z. Meng, Direct synthesis of DMC from CH_3OH and CO_2 over V-doped Cu–Ni/AC catalysts, Catal. Commun. 10 (2009) 1142–1145.
[18] J. Bian, M. Xiao, S.J. Wang, et al., Highly effective synthesis of dimethyl carbonate from methanol and carbon dioxide using a novel copper–nickel/graphite bimetallic nanocomposite catalyst, Chem. Eng. J. 147 (2009) 287–296.
[19] I. Omae, Aspects of carbon dioxide utilization, Catal. Today 115 (2006) 33–52.
[20] Y.J. Zhou, S.J. Wang, M. Xiao, et al., Novel Cu–Fe bimetal catalyst for the formation of dimethyl carbonate from carbon dioxide and methanol, RSC Adv. 2 (2012) 6831–6837.
[21] G. Jacobs, T.K. Das, Y.Q. Zhang, et al., Fischer–Tropsch synthesis: support, loading, and promoter effects on the reducibility of cobalt catalysts, Appl. Catal. A – Gen. 233 (2002) 263–281.
[22] W. Ma, E.L. Kugler, J. Wright, D.B. Dadyburjor, Mo–Fe catalysts supported on activated carbon for synthesis of liquid fuels by the Fischer–Tropsch process: effect of Mo addition on reducibility, activity, and hydrocarbon selectivity, Energy Fuels 20 (2006) 2299–2307.
[23] S.D. Qin, C.H. Zhang, J. Xu, et al., Effect of Mo addition on precipitated Fe catalysts for Fischer–Tropsch synthesis, J. Mol. Catal. A – Chem. 304 (2009) 128–134.
[24] R.M.M. Abbaslou, J. Soltan, A.K. Dalai, Iron catalyst supported on carbon nanotubes for Fischer–Tropsch synthesis: effects of Mo promotion, Fuel 90 (2011) 1139–1144.
[25] K. Faungnawakij, Y. Tanaka, N. Shimoda, et al., Hydrogen production from dimethyl ether steam reforming over composite catalysts of copper ferrite spinel and alumina, Appl. Catal. B – Environ. 74 (2007) 144–151.
[26] M. Aresta, A. Dibenedetto, E. Fracchiolla, et al., Mechanism of formation of organic carbonates from aliphatic alcohols and carbon dioxide under mild conditions promoted by carbodiimides. DFT calculation and experimental study, J. Org. Chem. 70 (2005) 6177–6186.